

## Supplementary Information

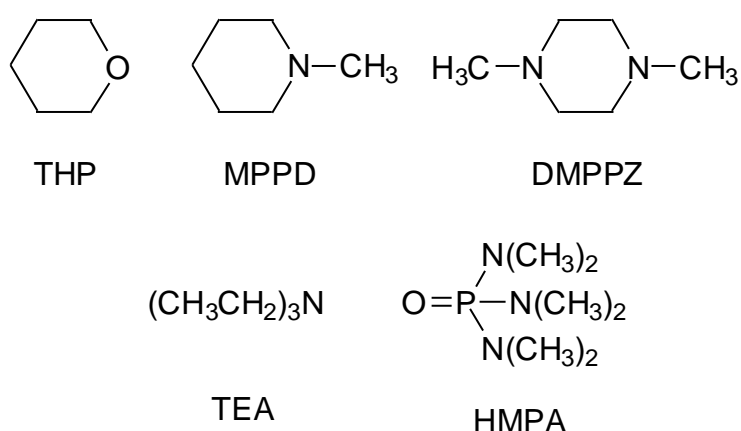
### Tuning Hydrogen Atom Abstraction from the Aliphatic C–H Bonds of Basic Substrates by Protonation. Control Over Selectivity by C–H Deactivation

Michela Salamone, Ilaria Giammarioli, and Massimo Bietti\*

*Dipartimento di Scienze e Tecnologie Chimiche, Università "Tor Vergata", Via della Ricerca Scientifica, 1 I-00133 Rome, Italy.*

<b>1) Chart of the substrates</b>	<b>S2</b>
<b>2) Stability studies</b>	<b>S2</b>
<b>3) Laser flash photolysis studies</b>	<b>S4</b>
<b>3.1) Time-resolved kinetic studies</b>	<b>S4</b>

## 1) Chart of the substrates



## 2) Stability studies

These studies were carried out at room temperature in nitrogen-saturated acetonitrile solutions containing dicumyl peroxide 10 mM and different amounts of TFA employing UV-Vis spectroscopy. The absorption spectra of acetonitrile solutions containing dicumyl peroxide and TFA, respectively, were recorded (spectra A and B) and their sum spectrum (A + B) was compared to the absorption spectrum recorded from a solution of dicumyl peroxide and TFA at the same concentrations of the individual spectra (spectrum C). The time evolution of spectrum C was then monitored. In Figures S1a and S2a, the sum spectra recorded from acetonitrile solutions containing dicumyl peroxide 10 mM and TFA (0.2 and 0.5 M, respectively, solid line), and the spectra recorded from acetonitrile solutions containing dicumyl peroxide 10 mM and TFA (0.2 and 0.5 M, respectively, circles) are compared showing in both cases excellent overlap. Figures S1b and S2b show the time evolution of the latter spectra. No significant spectral change was observed up to 60 minutes for  $[\text{TFA}] = 0.2 \text{ M}$  (Figure S1b), showing the stability of dicumyl peroxide under these experimental conditions. At  $[\text{TFA}] = 0.5 \text{ M}$ , partial decomposition of dicumyl peroxide was instead observed (Figure S2b).

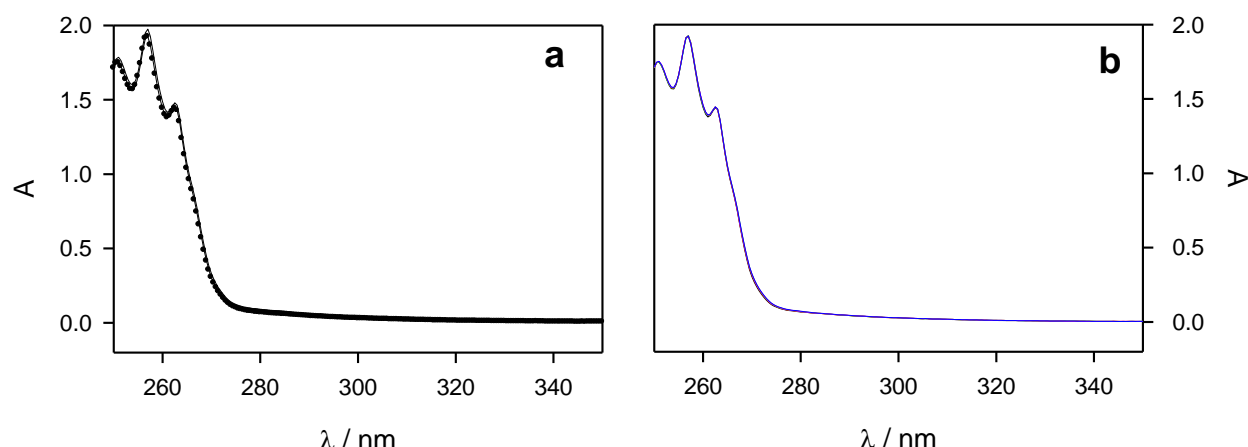


**Figure S1.** (a) Comparison between the absorption spectrum obtained from the sum of the spectra recorded from acetonitrile solutions containing dicumyl peroxide 10 mM and trifluoroacetic acid (TFA) 0.2 M (A + B, solid line), and the absorption spectrum obtained from an acetonitrile solution containing dicumyl peroxide 10 mM and TFA 0.2 M (C, circles). (b) Time-evolution of spectrum C monitored at 0, 15, 30, 45 and 60 minutes. Optical path of the cuvette = 0.5 cm.

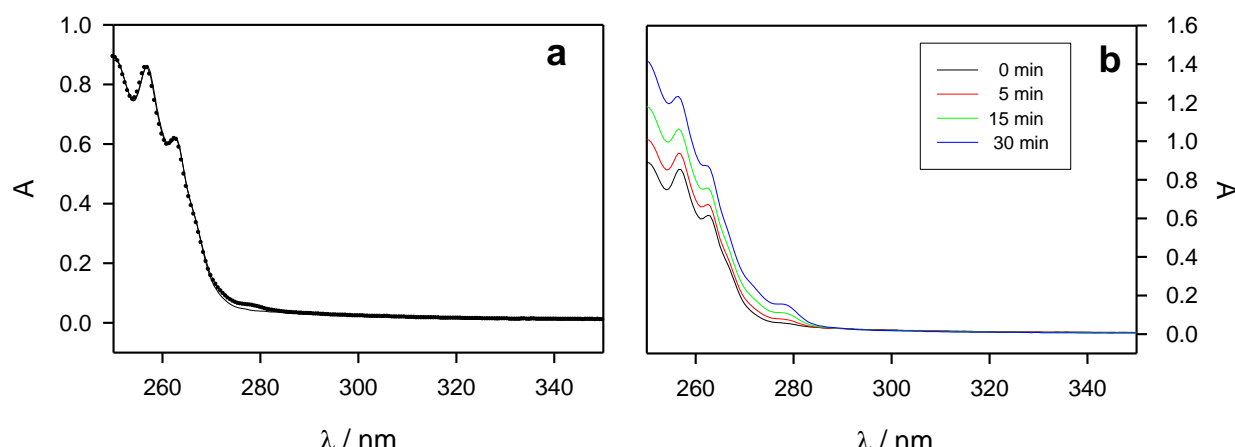


**Figure S2.** (a) Comparison between the absorption spectrum obtained from the sum of the spectra recorded from acetonitrile solutions containing dicumyl peroxide 10 mM and trifluoroacetic acid (TFA) 0.5 M (A + B, solid line), and the absorption spectrum obtained from an acetonitrile solution containing dicumyl peroxide 10 mM and TFA 0.5 M (C, circles). (b) Time-evolution of spectrum C monitored at 0, 5, 15 and 30 minutes. Optical path of the cuvette = 0.2 cm.

### 3) Laser flash photolysis studies

#### 3.1) Time resolved kinetic studies

##### $k_{\text{obs}}$ vs [substrate] plots for the reactions of CumO<sup>•</sup>

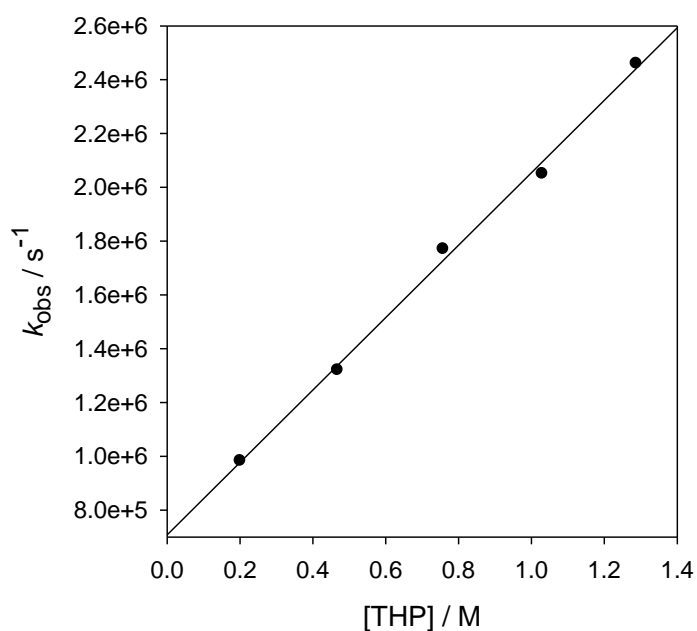


**Figure S3.** Plot of the observed rate constant ( $k_{\text{obs}}$ ) against [THP] for the reaction of the cumyloxy radical (CumO<sup>•</sup>, generated by 266 nm LFP from a 10 mM dicumyl peroxide solution) measured in nitrogen-saturated acetonitrile at  $T = 25$  °C, following the decay of CumO<sup>•</sup> at 490 nm. From the linear regression analysis: intercept =  $7.08 \times 10^5 \text{ s}^{-1}$ ,  $k_{\text{H}} = 1.35 \times 10^6 \text{ M}^{-1}\text{s}^{-1}$ ,  $r^2 = 0.9968$ .

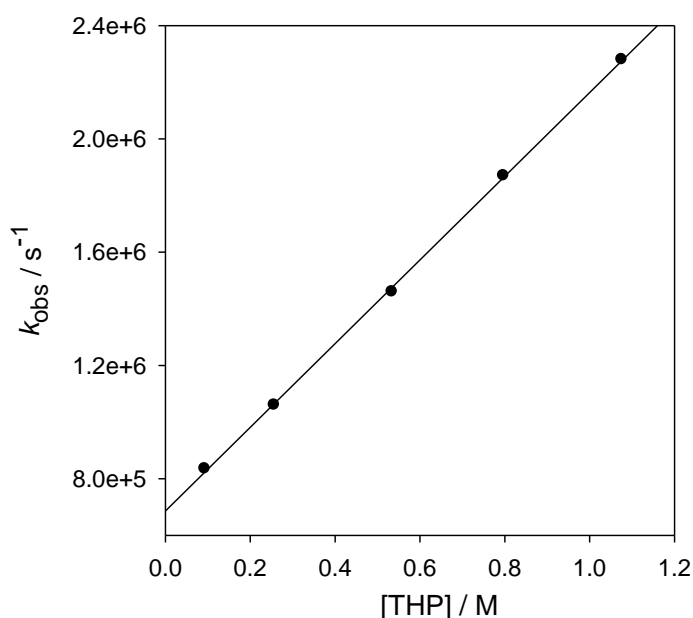


**Figure S4.** Plot of the observed rate constant ( $k_{\text{obs}}$ ) against [THP] for the reaction of the cumyloxy radical ( $\text{CumO}^{\bullet}$ , generated by 266 nm LFP from a 10 mM dicumyl peroxide solution) measured in nitrogen-saturated acetonitrile containing 0.1 M TFA at  $T = 25$  °C, following the decay of  $\text{CumO}^{\bullet}$  at 490 nm. From the linear regression analysis: intercept =  $6.86 \times 10^5 \text{ s}^{-1}$ ,  $k_{\text{H}} = 1.48 \times 10^6 \text{ M}^{-1}\text{s}^{-1}$ ,  $r^2 = 0.9997$ .

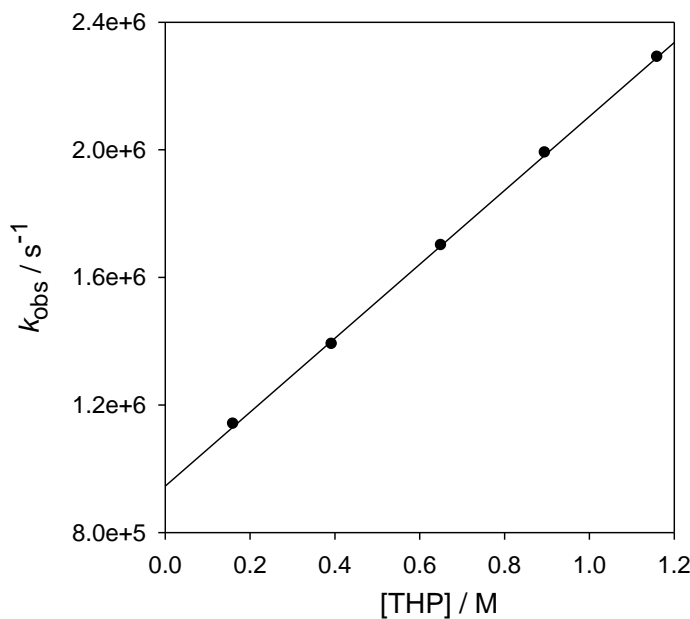


**Figure S5.** Plot of the observed rate constant ( $k_{\text{obs}}$ ) against [THP] for the reaction of the cumyloxy radical ( $\text{CumO}^{\bullet}$ , generated by 266 nm LFP from a 10 mM dicumyl peroxide solution) measured in nitrogen-saturated acetonitrile containing 3.5 M AcOH at  $T = 25$  °C, following the decay of  $\text{CumO}^{\bullet}$  at 490 nm. From the linear regression analysis: intercept =  $9.46 \times 10^5 \text{ s}^{-1}$ ,  $k_{\text{H}} = 1.16 \times 10^6 \text{ M}^{-1}\text{s}^{-1}$ ,  $r^2 = 0.9997$ .

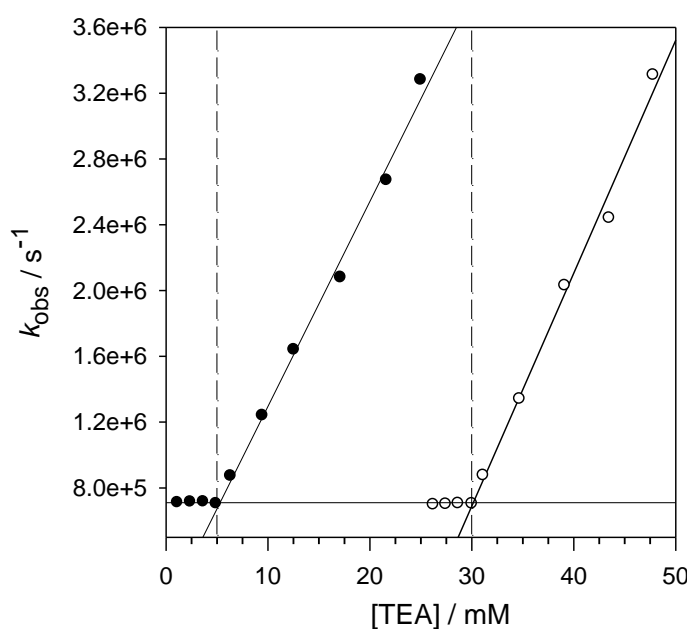


**Figure S6.** Plot of the observed rate constant ( $k_{\text{obs}}$ ) against [TEA] for reaction of the cumyloxy radical ( $\text{CumO}^{\bullet}$ , generated by 266 nm LFP from a 10 mM dicumyl peroxide solution) measured at  $T = 25^{\circ}\text{C}$  in a nitrogen-saturated MeCN solution containing TFA 5 mM (black circles) and 30 mM (white circles), by following the decay of  $\text{CumO}^{\bullet}$  at 490 nm. From the linear regression analysis: [TFA] = 5 mM, in the 5-25 mM [TEA] range:  $k_{\text{H}} = 1.25 \times 10^8 \text{ M}^{-1}\text{s}^{-1}$ ,  $r^2 = 0.9922$ ; [TFA] = 30 mM, in the 30-48 mM [TEA] range:  $k_{\text{H}} = 1.42 \times 10^8 \text{ M}^{-1}\text{s}^{-1}$ ,  $r^2 = 0.9892$ .

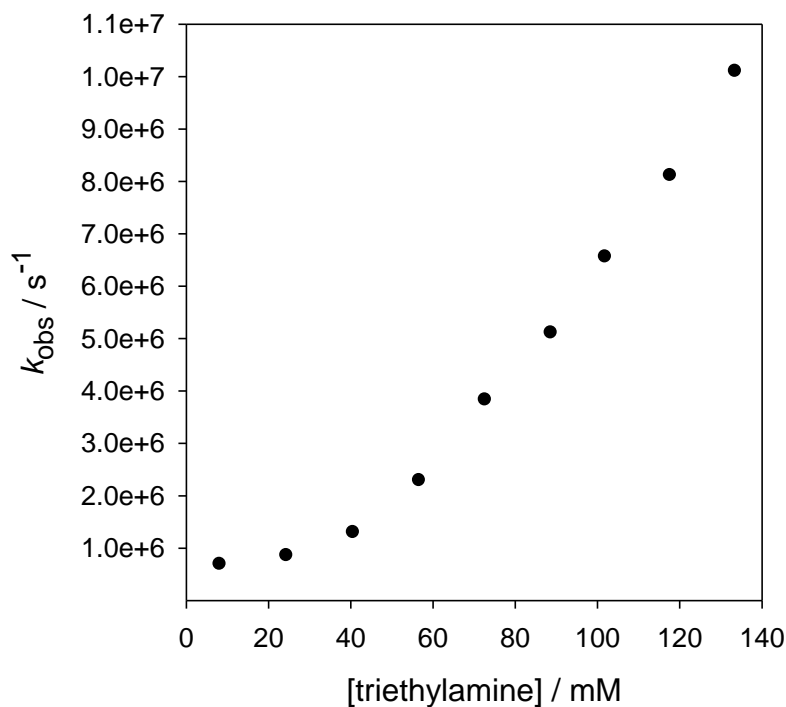


**Figure S7.** Plot of the observed rate constant ( $k_{\text{obs}}$ ) against [TEA] for the reaction of the cumyloxy radical ( $\text{CumO}^{\bullet}$ , generated by 266 nm LFP from a 10 mM dicumyl peroxide solution) measured in nitrogen-saturated acetonitrile containing 0.1 M AcOH at  $T = 25^{\circ}\text{C}$ , following the decay of  $\text{CumO}^{\bullet}$  at 490 nm.

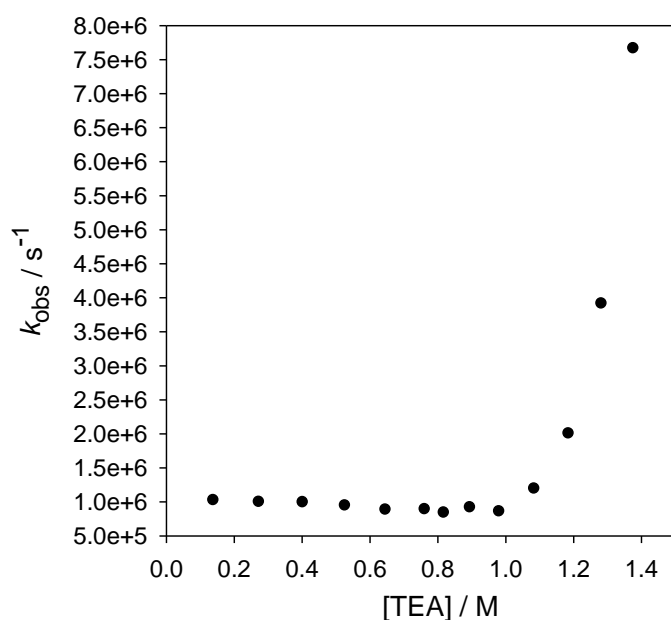


**Figure S8.** Plot of the observed rate constant ( $k_{\text{obs}}$ ) against [TEA] for the reaction of the cumyloxy radical ( $\text{CumO}^{\bullet}$ , generated by 266 nm LFP from a 10 mM dicumyl peroxide solution) measured in nitrogen-saturated acetonitrile containing 3.5 M AcOH at  $T = 25$  °C, following the decay of  $\text{CumO}^{\bullet}$  at 490 nm.

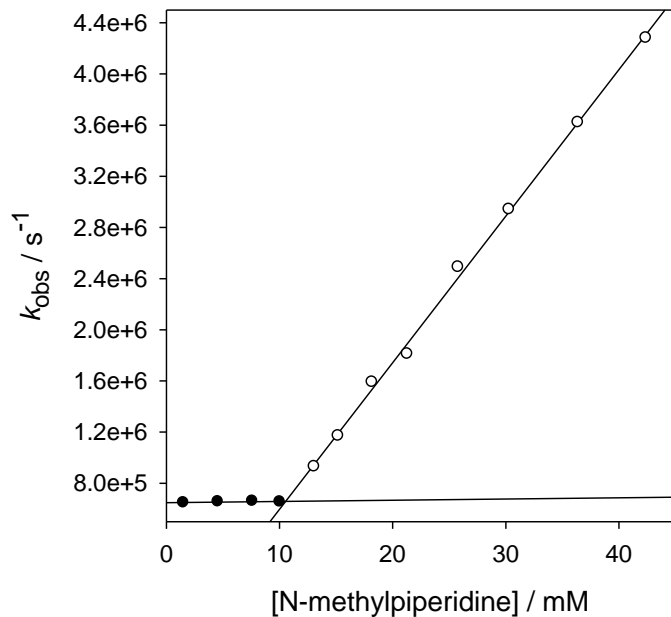


**Figure S9.** Plot of the observed rate constant ( $k_{\text{obs}}$ ) against [MPPD] for the reaction of the cumyloxy radical ( $\text{CumO}^{\bullet}$ , generated by 266 nm LFP from a 10 mM dicumyl peroxide solution) measured in nitrogen-saturated acetonitrile containing 10 mM TFA at  $T = 25$  °C, following the decay of  $\text{CumO}^{\bullet}$  at 490 nm. From the linear regression analysis in the 10-42 mM [MPPD] range:  $k_{\text{H}} = 1.15 \times 10^8 \text{ M}^{-1} \text{ s}^{-1}$ ,  $r^2 = 0.9982$ .

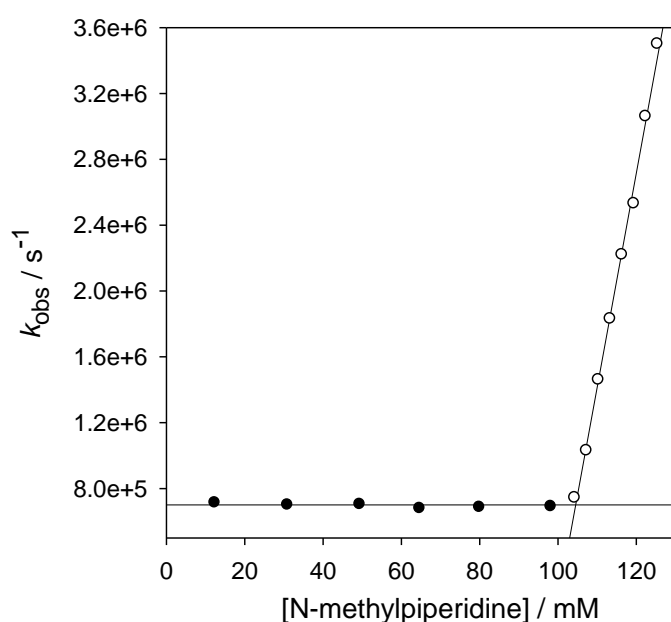


**Figure S10.** Plot of the observed rate constant ( $k_{\text{obs}}$ ) against [MPPD] for the reaction of the cumyloxy radical ( $\text{CumO}^{\bullet}$ , generated by 266 nm LFP from a 10 mM dicumyl peroxide solution) measured in nitrogen-saturated acetonitrile containing 100 mM TFA at  $T = 25$  °C, following the decay of  $\text{CumO}^{\bullet}$  at 490 nm. From the linear regression analysis in the 100-125 mM [MPPD] range:  $k_{\text{H}} = 1.30 \times 10^8 \text{ M}^{-1} \text{ s}^{-1}$ ,  $r^2 = 0.9960$ .

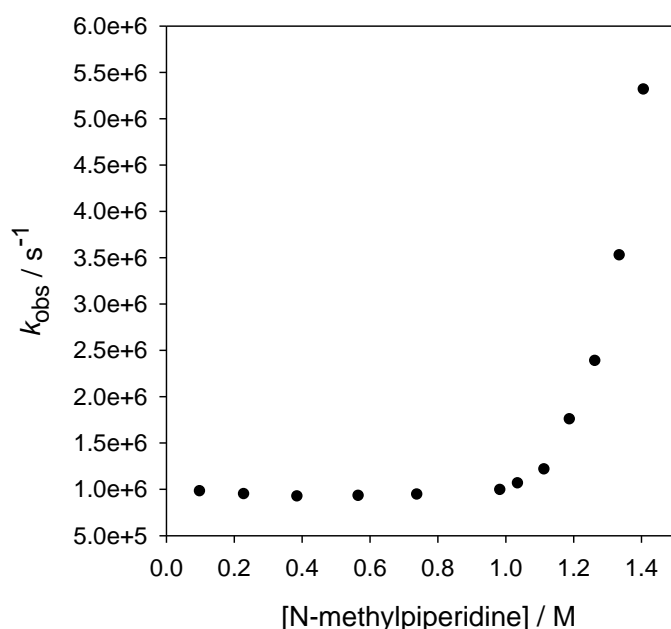


**Figure S11.** Plot of the observed rate constant ( $k_{\text{obs}}$ ) against [MPPD] for the reaction of the cumyloxy radical ( $\text{CumO}^{\bullet}$ , generated by 266 nm LFP from a 10 mM dicumyl peroxide solution) measured in nitrogen-saturated acetonitrile containing 3.5 M AcOH at  $T = 25$  °C, following the decay of  $\text{CumO}^{\bullet}$  at 490 nm.

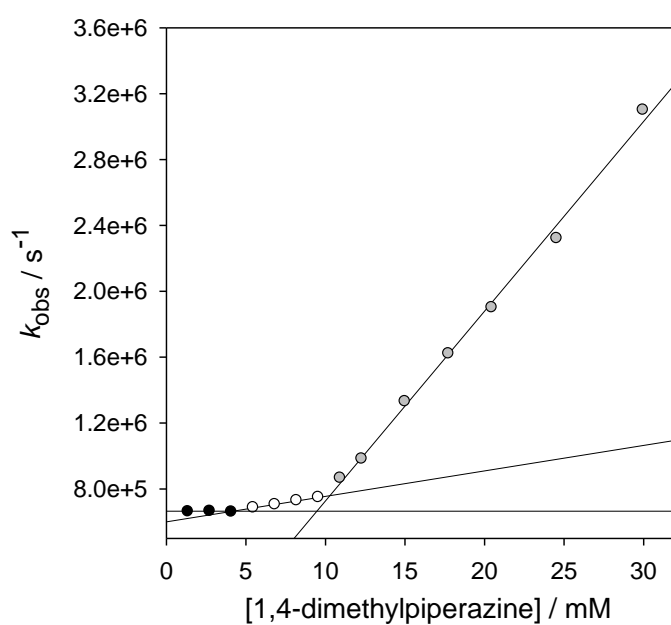


**Figure S12.** Plots of the observed rate constant ( $k_{\text{obs}}$ ) against [DMPPZ] for reaction of the cumyloxy radical (CumO $^{\bullet}$ ) measured at  $T = 25$  °C in a nitrogen-saturated MeCN solution containing 10 mM TFA, by following the decay of CumO $^{\bullet}$  at 490 nm. From the linear regression analysis: in the 5-10 mM [DMPPZ] range:  $k_{\text{H1}} = 1.55 \times 10^7 \text{ M}^{-1} \text{ s}^{-1}$ ,  $r^2 = 0.9963$ ; in the 10-30 mM [DMPPZ] range:  $k_{\text{H2}} = 1.15 \times 10^8 \text{ M}^{-1} \text{ s}^{-1}$ ,  $r^2 = 0.9961$ .

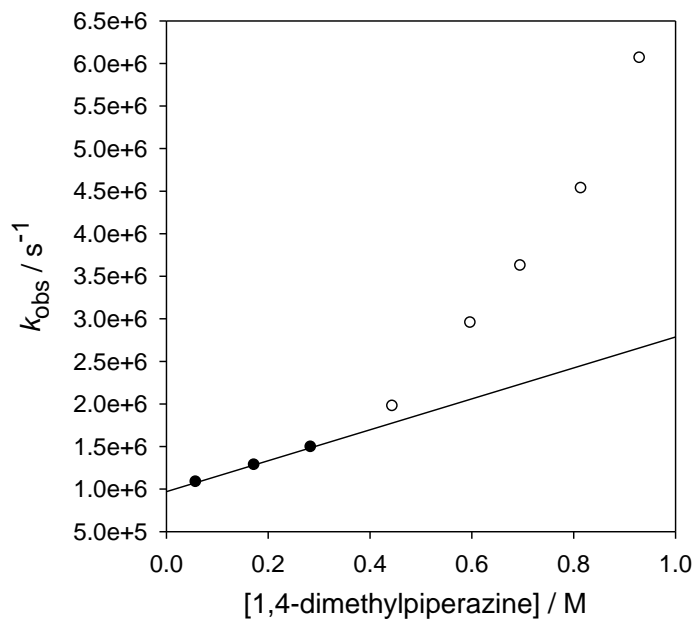


**Figure S13.** Plot of the observed rate constant ( $k_{\text{obs}}$ ) against [DMPPZ] for the reaction of the cumyloxy radical (CumO $^{\bullet}$ , generated by 266 nm LFP from a 10 mM dicumyl peroxide solution) measured in nitrogen-saturated acetonitrile containing 3.5 M AcOH at  $T = 25$  °C, following the decay of CumO $^{\bullet}$  at 490 nm. From the linear regression analysis in the 0-0.3 M [DMPPZ] range:  $k_{\text{H}} = 1.82 \times 10^6 \text{ M}^{-1} \text{ s}^{-1}$ ,  $r^2 = 0.9995$ .

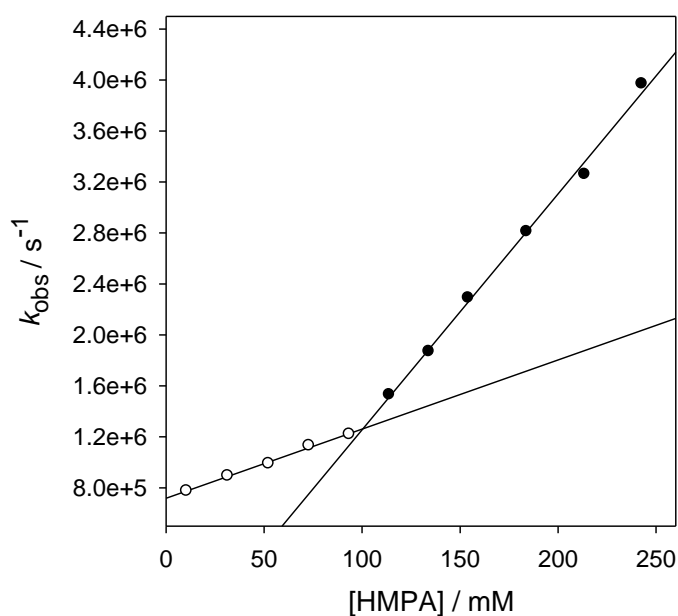


**Figure S14.** Plots of the observed rate constant ( $k_{\text{obs}}$ ) against [HMPA] for reaction of the cumyloxy radical ( $\text{CumO}^{\bullet}$ ) measured at  $T = 25$  °C in a nitrogen-saturated MeCN solution containing 100 mM TFA, by following the decay of  $\text{CumO}^{\bullet}$  at 490 nm. From the linear regression analysis: in the 0-100 mM [HMPA] range:  $k_{\text{H1}} = 5.43 \times 10^6 \text{ M}^{-1} \text{ s}^{-1}$ ,  $r^2 = 0.9963$ ; in the 100-243 mM [HMPA] range:  $k_{\text{H2}} = 1.85 \times 10^7 \text{ M}^{-1} \text{ s}^{-1}$ ,  $r^2 = 0.9961$ .

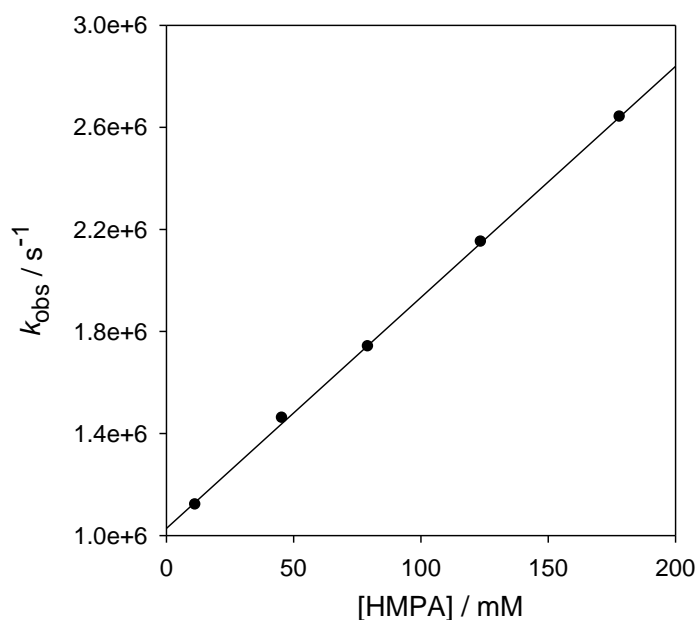


**Figure S15.** Plot of the observed rate constant ( $k_{\text{obs}}$ ) against [HMPA] for the reaction of the cumyloxy radical ( $\text{CumO}^{\bullet}$ , generated by 266 nm LFP from a 10 mM dicumyl peroxide solution) measured in nitrogen-saturated acetonitrile containing 3.5 M AcOH at  $T = 25$  °C, following the decay of  $\text{CumO}^{\bullet}$  at 490 nm. From the linear regression analysis: intercept =  $1.03 \times 10^6 \text{ s}^{-1}$ ,  $k_{\text{H}} = 9.06 \times 10^6 \text{ M}^{-1} \text{ s}^{-1}$ ,  $r^2 = 0.9996$ .